Spectroscopic and Transient Kinetic Studies of Site Requirements in Iron-Catalyzed Fischer−Tropsch Synthesis

Senzi Li,[†] Weiping Ding,[†,‡] George D. Meitzner,[§] and Enrique Iglesia*[,†]

Department of Chemical Engineering, University of California, Berkeley, California 94720

Received: May 16, 2001; In Final Form: October 15, 2001

The structure, reduction/carburization, and catalytic performance of K- and Cu-promoted Fe_2O_3 during initial contact with synthesis gas were examined by combining kinetic analysis of the initial stages of Fischer−Tropsch synthesis (FTS) with X-ray absorption spectroscopy. Oxygen removal initially occurs without FTS reactions as Fe_2O_3 is reduced to inactive oxygen-deficient Fe_2O_3 species. Hydrocarbon synthesis reactions become detectable only as Fe_3O_4 forms and rapidly converts to FeC_x. FTS reactions require only the incipient conversion of the surface layers to a dynamic and active surface phase, which consists of FeC_x with steady-state surface coverages of vacancies, formed via oxygen and carbon removal during the formation of monomers, CO_2, and H_2O. Such surfaces tend to respond to changes in the contacting gas phase within turnover times by changing the relative surface concentration of carbon, oxygen, CO, and hydrogen. The catalytic behavior of these dynamic surfaces is largely independent of the carbide or oxide nature of the particle cores. These findings, combined with the rapid formation and interconversion of Fe_3O_4 and FeC_x within characteristic FTS turnover times, make the definite assignment of FTS activity to either phase neither appropriate nor kinetically rigorous. The presence of K and Cu increases FTS rates, and the steady-state extent of carburization by providing nucleation sites for the formation of smaller FeC_x crystallites. These smaller active domains lead, in turn, to shorter diffusion paths and to a larger number of sites for CO adsorption/dissociation and for FTS reactions. These structural promotion effects of K and Cu were consistent with reaction rates, X-ray absorption spectra, and site density measured on promoted and unpromoted catalysts as a function of time in contact with synthesis gas.

Introduction

Precipitated Fe−Zn oxide precursors promoted with K and Cu form active and selective Fischer−Tropsch synthesis catalysts[1] after activation processes that lead to complex mixtures of reduced Fe compounds. The structure of these catalyst precursors and their reduction in H_2 and carburization in CO were previously examined with specific emphasis on the role of the K and Cu promoters on the structure and transformations of these materials.[2]

The objective of the present study is to characterize these structural changes, the stoichiometry of the active phases formed, and their catalytic behavior as Fischer−Tropsch synthesis reactions occur. The reduction and carburization kinetics in H_2−CO mixtures, the rate of hydrocarbon synthesis reactions, and the density of active sites on K/Cu-promoted Fe_2O_3 were probed using a combination of isothermal rate transients and X-ray absorption spectroscopy during the initial contact of these samples with synthesis gas. The products formed during initial exposure to synthesis gas were detected using on-line mass spectrometric analysis combined with deconvolution methods required in order to unravel the concentrations of individual components from complex fragmentation patterns of multicomponent hydrocarbon mixtures. These methods allowed concurrent measurements of the amount of oxygen removed from Fe_2O_3 precursors and of the effect of oxygen-deficiency on FTS rates. X-ray absorption spectroscopic measurements were carried out in parallel at identical reaction conditions in order to detect the evolution of Fe, FeO_y, and FeC_x structures during FTS. These studies were combined with measurements of the density of CO binding sites using recently developed protocols[3] and of BET surface areas after quenching samples during FTS reactions.

The observed correlation between the transient evolution of the catalyst structure and of the reaction products, showed that the surface areas of particles with Fe_3O_4 or FeC_x composition in near surface layers controls FTS rates, irrespective of the chemical nature of the residual oxide or carbide cores. These findings, combined with site density values inferred from surface area and CO chemisorption, show that K and Cu provide sites for the rapid nucleation of a high density of Fe_3O_4 and FeC_x clusters, a process that leads to the ultimate formation of smaller and more extensively carburized catalytic structures, with a higher surface area and a larger number of active sites for FTS reactions.

In these studies, structural promoters, such as ZnO[1,4] or SiO_2,[5,6] were excluded from Fe oxide precursors in order to discern the specific effects of Cu and K, without the structural complexity introduced by additional promoters. These structural promoters increase the surface areas of Fe oxide precursors, without detectable changes in the nature of the active sites or in chain growth pathways.[2] ZnO increases surface areas but also forms a $ZnFe_2O_4$ phase, which does not reduce or carburize

---

* To whom correspondence should be addressed. E-mail: iglesia@cchem.berkeley.edu.

[†] Department of Chemical Engineering, University of California, Berkeley.

[‡] Current Address: Department of Chemistry, Nanjing University, Nanjing, China.

[§] Edge Analytical, Inc., Middleton, WI 53562.

10.1021/jp0118827 CCC: $22.00

during FTS, as shown by Zn K-edge X-ray absorption spectroscopy.[8] The behavior of Fe oxides promoted by ZnO has been reported separately.[9] The exclusion of Zn from the Fe−K−Cu oxides used here does not influence the nature of the structural transformations or the way in which they are influenced by Cu or K.

Experimental Section

1. Synthesis of Fe−K−Cu Oxide Precursors. Fe_2O_3 precursors were prepared by precipitation from aqueous solutions of $Fe(NO_3)_3$ (Aldrich, >99.9%, 3.0 M). These solutions were added at 0.033 cm^3/s into a continuously stirred flask maintained at 353 K and initially containing deionized water (50 cm^3). Ammonium carbonate [$(NH_4)_2CO_3$; Aldrich, 99.9%, 1 M] was added separately into this flask; its flow rate was adjusted in order to maintain the slurry pH at 7.0 ± 0.1 (pH Meter; Omega, PHB-62). The resulting precipitates (∼20 g) were washed five times with deionized water (1 *li*/g) and dried in ambient air at 393 K overnight. The dry powders were treated in flowing dry air (∼500 cm^3/h•g-cat.) at 623 K for 1 h and then impregnated to incipient wetness with aqueous solutions of K_2CO_3 (Aldrich, 99.99%, 0.16 M) and/or $Cu(NO_3)_2$ (Aldrich, 99.99%, 0.16 M) to give the desired K/Fe and Cu/Fe atomic ratios (K/Fe = 0.02, Cu/Fe = 0.01). The samples were dried again in ambient air at 373 K overnight and treated in dry air at 673 K for 4 h; this treatment leads to the decomposition of nitrates, hydroxides and carbonates, except K_2CO_3.[10] The resulting catalyst precursors contained CuO, Fe_2O_3, and K_2CO_3 and they are designated as Fe_2O_3, Fe_2O_3−Cu, Fe_2O_3−K, and Fe_2O_3−K−Cu. They were uniaxially pressed into pellets at 440 MPa, and sieved to retain particles with 100−180 μm diameter, which were used in all catalytic and characterization studies.

2. Structural and Chemical Characterization of Precursors and Catalysts. *2.1. Isothermal Transient Measurements of Fischer−Tropsch Synthesis Rates.* Initial rates of reduction and carburization of Fe oxide precursors and their residual oxygen content during FTS were measured using on-line mass spectrometry (Leybold Inficon, Transpector Series) as a function of time of contact with synthesis gas. Samples (0.2 g) were held within a quartz microreactor and diluted with graphite (0.5 g, Alfa AESAR, 99.998%, 100∼180 μm, BET surface area < 1 m^2/g) to minimize temperature gradients during FTS and to reproduce the exact details of the X-ray absorption studies conducted in parallel, in which graphite was used as a diluent in order to minimize absorption artifacts. The inertness of graphite during FTS was confirmed by the absence of CO, CO_2, or any hydrocarbons even at 873 K in flowing H_2. These products could form via hydrogenation of graphite or of CO_x formed by solid-state reactions of carbon with lattice oxygen in Fe oxide precursors or intermediates. Samples were treated in He (0.268 mol/h) at 573 K for 0.2 h, cooled to 523 K, and then exposed to synthesis gas (H_2/CO/Ar = 2/1/2, 100 kPa, 0.268 mol/h). The transient evolution of hydrocarbons formed in FTS reactions and of reduction-carburization products (CH_4, H_2O, and CO_2, etc.) was measured at 523 K as a function of time using on-line mass spectrometry (Leybold Inficon, Transpector Series, 1.02 s/scan at 32 ms dwell time).

These isothermal transient measurements were also carried out on Fe_3O_4 and FeC_x (a mixture of $Fe_{2.5}C$ and Fe_3C) samples prepared by temperature-programmed reactions of Fe_2O_3 in H_2 or CO, respectively. The synthetic procedures used to prepare these materials involved interrupted thermal treatments of Fe_2O_3 precursors and verification of the structural purity of the phases formed by X-ray diffraction. These Fe_3O_4 and FeC_x powders were prepared from Cu-containing Fe_2O_3 precursors, because Cu leads to the easier isolation of pure Fe_3O_4, without residual Fe_2O_3 and without the formation of FeO or Fe. The Fe_2O_3−Cu precursor (0.2 g, Cu/Fe = 0.01) was treated in 20% H_2/Ar (0.268 mol/h) as the temperature was increased to 533 K at 0.083 K/s; this procedure led to the stoichiometric reduction of Fe_2O_3−CuO to pure Fe_3O_4 and Cu metal. This was confirmed by the oxygen removal stoichiometry and by X-ray diffraction. FeC_x-Cu was prepared by treating Fe_2O_3−CuO (0.2 g, Cu/Fe = 0.01) precursors in 20% CO/Ar (0.268 mol/h), whereas increasing the temperature to 673 K at 0.083 K/s. The slow ramping rate was used in order to accurately interrupt the structural transformation before deposition of noncarbidic carbon. X-ray diffraction measurements confirmed that prereduced samples consisted of pure Fe_3O_4, whereas carburized samples contained a mixture of $Fe_{2.5}C$ and Fe_3C, which we denote here as FeC_x. Pre-reduced and pre-carburized samples were cooled to 523 K in He (0.268 mol/h) and exposed to synthesis gas for isothermal transient measurements without intervening exposure to ambient air.

2.2. X-ray Absorption Spectroscopy (XAS) Measurements. X-ray absorption spectra were collected at the Fe K-edge using a wiggler side-station beamline (4−1) at the Stanford Synchrotron Radiation Laboratory (SSRL). The storage ring was operated at 30−100 mA and 3.0 GeV during the measurements. Two Si(111) crystals detuned by 20% in order to reject harmonics were used in the monochromator. The most restrictive aperture along the beam path was a 0.2 × 12 mm slit, which limited the energy resolution to ∼1 eV at the Fe K-edge (7.112 keV).[11,12] The spectra were analyzed using WinXAS (version 1.2).[13] Principal component analysis[14] and linear combination methods[15] were used in order to determine the structures present in each sample from spectral features in the near-edge region (7.090−7.240 keV). All samples were diluted to 15 wt % Fe using graphite powder (Alfa AESAR, 99.9995%, BET surface area $S_g < 1$ m^2/g), pressed at 300 MPa, sieved to retain 100−180 μm particles, and placed within a quartz X-ray absorption capillary cell.[3] After exposure to synthesis gas (H_2/CO = 2) for a given period of time at 523 K, He was used to flush the samples, which were cooled to ambient temperature in 10 s by removing the surrounding heated Cu block. X-ray absorption spectra were measured in flowing He at ambient temperature.

2.3. CO Chemisorption and Surface Area Measurements. CO chemisorption uptakes were measured after transient experiments in synthesis gas at 523 K for 1 h and a subsequent He purge (0.268 mol/h) at 523 K for 1 h; the purge step was used in order to remove reversibly adsorbed species. CO chemisorption and BET surface area measurements were then carried out after cooling to ambient temperature. The details of these CO chemisorption procedures have been described elsewhere.[3] BET surface area measurements were carried out after FTS reaction at 523 K for 1 h, quenching to ambient temperature, and passivation of the samples in flowing 1% O_2/He at room temperature. N_2 physisorption measurements were performed at its normal boiling point (77 K) using an Autosorb 6 system (Quantachrome, Inc.). Surface areas were calculated using the BET method.

Results and Discussion

Product Evolution and X-ray Absorption Measurements during Isothermal Transients of Fe_2O_3 in Synthesis Gas. Figure 1 shows the rates of formation of CH_4, H_2O, and CO_2 during initial contact of Fe_2O_3 with H_2/CO at 523 K. During the first 140 s, lattice oxygen was removed from Fe_2O_3 as CO_2

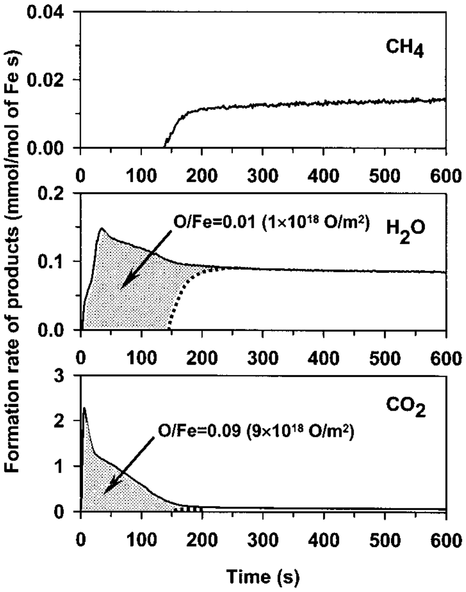

Figure 1. Rates of formation of CH_4, H_2O, and CO_2 as a function of time during contact with synthesis gas at 523 K for precipitated Fe_2O_3 (0.2 g sample; $H_2/CO = 2$, synthesis gas flow rate = 0.268 mol/h). The shaded areas in the formation of H_2O and CO_2 are their respective amounts formed from the reduction of Fe oxides upon exposure to synthesis gas; the dashed lines are their expected values from subsequent FTS reactions.

and H_2O, without the concurrent formation of CH_4. Here, CH_4 formation rates are used as a surrogate measure of hydrocarbon synthesis rates, because CH_4 concentrations can be measured accurately and they change with time in parallel with those of heavier hydrocarbon products. CH_4 formation became detectable after an induction period and it rapidly reached steady-state (<200 s). Thus, the formation of the active sites required for FTS reactions is rapid and it requires the initial removal of only a very small amount of lattice oxygen (~7%) from Fe_2O_3. It appears that the number of sites and the surface area available for FTS reactions, as well as the surface composition of the active phase reach near steady-state values after the removal of only a few equivalent monolayers of lattice oxygen from Fe_2O_3 precursors.

The lattice oxygen atoms are removed from Fe_2O_3 precursors by H_2 to form H_2O or by CO to form CO_2. The O/Fe atomic ratios for the lattice oxygen removed as H_2O and CO_2 are 0.01 and 0.09, respectively (the shaded area under the initial reduction peaks in Figure 1), which corresponds to a total sum of oxygen removed relative to Fe (O/Fe) of 0.1. This corresponds to 1.5×10^{19} O-atom/m^2 for the BET surface area of these precursor oxides (~50 m^2/g). This value is similar to the oxygen surface density expected for oxygen-exposed metal oxide surfaces (~10^{19} O-atom/m^2). CO appears to be the preferred reductant and CO_2 the predominant product for pure Fe_2O_3. Steady-state FTS reaction rates required the removal of some lattice oxygen from stoichiometric Fe_2O_3, which appears not to be able to catalyze FTS reactions without some reduction. Active sites require the formation of oxygen-deficient species (Fe_2O_{3-x}, x~0.2). These stoichiometries, however, clearly represent average values for Fe_2O_3 crystallites, and they reflect a substantially unreduced Fe_2O_3 core surrounded by more extensively reduced and carburized regions near particle surfaces. FTS rates reached steady-state values after structural changes in only a few outer layers of the Fe_2O_3 precursor crystallites.

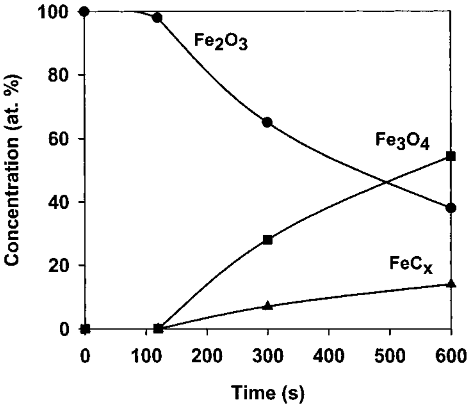

Figure 2. Structural evolution of Fe_2O_3 with time on stream after exposure to synthesis gas at 523 K: (●) Fe_2O_3, (■) Fe_3O_4, and (▲) FeC_x (1 mg sample; $H_2/CO = 2$, synthesis gas flow rate = 107 mol/mol of Fe h).

These transient studies are unable to detect the additional reduction and carburization events that occur after attaining steady-state FTS rates because the amounts of H_2O and CO_2 formed in FTS reactions become significantly larger than those formed via the gradual removal of additional lattice oxygen from less accessible internal regions within Fe_2O_3 crystallites. To detect structural changes occurring over these longer time scales, X-absorption spectroscopy was used to measure the structural evolution of Fe_2O_3 after exposure to synthesis gas at FTS reaction conditions (523 K, $H_2/CO = 2$) for various periods of times.

Principal component analysis methods[14] identified three components, Fe_2O_3, Fe_3O_4, and FeC_x, as the only species that changed in concentration as the near-edge X-ray absorption spectra changed with time on stream. The two Fe carbide phases (Fe_3C and $Fe_{2.5}C$) cannot be distinguished by their near-edge spectra and they are reported as a lump and denoted as FeC_x. The spectra of samples were described as linear combinations of the near-edge spectra of the three standard compounds identified by principal component analysis.[15] The detailed analysis procedure has been described elsewhere[3]. Figure 2 shows the change in the concentrations of the Fe_2O_3, Fe_3O_4, and FeC_x phases as a function of the time elapsed after initial contact with synthesis gas at 523 K. Neither Fe_3O_4 nor FeC_x components were detected during the induction period. After the induction period, Fe_3O_4 and FeC_x formed concurrently and the extent of carburization increased gradually with time. Thus, it appears that the O-deficient Fe_2O_3 initially formed undergoes structural changes to form species with the local coordination of Fe_3O_4 only when the density of oxygen vacancies in Fe_2O_3 reaches a critical value, which destabilizes the Fe_2O_3 structure and leads to the nucleation of the Fe_3O_4 phase.

Fe_3O_4 was never detected without the concurrent presence of FeC_x during exposure to synthesis gas, suggesting that its subsequent conversion to FeC_x occurs at rates similar to its rate of formation from Fe_2O_3 in synthesis gas at 523 K. The simultaneous appearance of Fe_3O_4 and FeC_x coincides with the detection of gas-phase hydrocarbon products, suggesting that Fe_3O_4, FeC_x, or both, provide the required catalytic sites. As Fe_3O_4 continued to convert to FeC_x, FTS reaction rates remained nearly constant, even as the structures changed markedly, suggesting that only a fraction of the Fe species, probably those near surfaces, are involved in FTS reactions and that they form rapidly during initial contact with synthesis gas. Clearly, the structure and composition of near-surface layers are more likely to influence catalytic turnovers than the structure of an inaccessible bulk; the easier access by reactants to near-surface regions also lead these regions to reach steady-state compositions

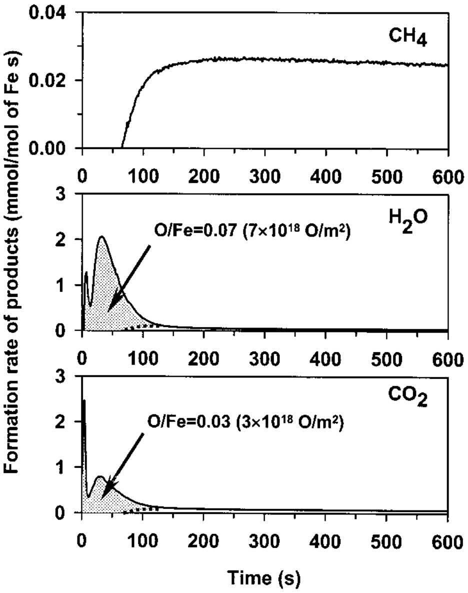

Figure 3. Rates of formation of CH_4, H_2O, and CO_2 as a function of time during contact with synthesis gas at 523 K for Fe_2O_3−Cu (0.2 g sample; Cu/Fe = 0.01; $H_2/CO = 2$, synthesis gas flow rate = 0.268 mol/h). The shaded areas in the formation of H_2O and CO_2 are their respective amounts formed from the reduction of Fe oxides upon exposure to synthesis gas; the dashed lines are their expected values from subsequent FTS reactions.

and structures much more rapidly than particle cores, which are also probed by X-ray photons, but which are accessible only via bulk diffusion of oxygen and carbon. FTS reaction rates on such steady-state surfaces are not influenced by the residual presence of an Fe_2O_3 or Fe_3O_4 core within particles or by the gradual conversion of these cores to FeC_x during more extended contact with synthesis gas.

Product Evolution and X-ray Absorption Measurements during Exposure of Fe_2O_3-Cu to Synthesis Gas. Figure 3 shows the rates of lattice oxygen removal and of CH_4 formation on Fe_2O_3−Cu (Cu/Fe = 0.01) during initial exposure to synthesis gas at 523 K. The transient evolution of products on Fe_2O_3−Cu resembles that observed on pure Fe_2O_3, except that the induction period is significantly shorter and lattice oxygen is predominately removed by H_2 as H_2O, instead of by CO. CuO reduces to Cu metal in H_2 at 453 K,[2] and the area under the sharp first peak in Figure 3 corresponds to the removal of all lattice oxygen atoms from CuO to form Cu metal. Cu appears to increase the rate of Fe_2O_3 reduction to Fe_3O_4 by providing H_2 dissociation sites; consequently, a larger number of oxygen atoms are removed by H_2 (O/Fe = 0.07) as H_2O, than by CO (O/Fe = 0.03) as CO_2 on Fe_2O_3−Cu. The total number of oxygen atoms removed during the induction period required in order to reach steady-state FTS rates, however, was very similar to that on pure Fe_2O_3, even though the presence of Cu increased reduction rates and provided alternate reduction pathways. CH_4 formation rates increased as oxygen was removed after the initial induction period, and then reached steady-state rates after ∼150 s. Cu increases the rate of oxygen removal and the rate of formation of active sites; as a result, Cu also decreases the time required in order to reach the catalytic steady-state. Cu leads to higher steady-state FTS reaction rates; even though both Fe_2O_3 and Fe_2O_3−Cu reached similar extents of reduction, as measured by the amount of oxygen removed during the induction period. Cu appears to lead to the formation of a higher density of active sites, a conclusion consistent with the measured number of CO binding sites after activation and FTS reactions on Fe_2O_3 and Fe_2O_3−Cu samples, as discussed below. It appears that the formation of Cu metal crystallites on Fe_2O_3 crystallite surfaces during the early stages of reaction with synthesis gas leads to the rapid nucleation of a higher density of Fe_3O_4 and FeC_x crystallites. The resulting larger number of nuclei leads to the ultimate formation of smaller crystallites of either Fe_3O_4 or FeC_x, to larger active surface areas, and to higher FTS rates.

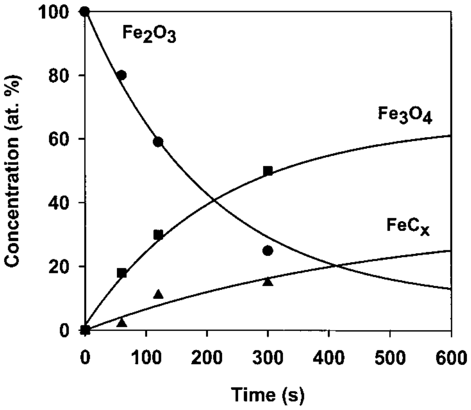

Figure 4. Structural evolution of Fe_2O_3−Cu with time on stream after exposure to synthesis gas at 523 K: (●) Fe_2O_3, (■) Fe_3O_4, and (▲) FeC_x (1 mg sample; Cu/Fe = 0.01; $H_2/CO = 2$, synthesis gas flow rate = 107 mol/mol of Fe h).

Figure 4 shows the results of a linear combination analysis of the near-edge spectra measured during exposure of Fe_2O_3−Cu to synthesis gas at 523 K. Fe_2O_3−Cu underwent sequential structural changes very similar to those detected in Fe_2O_3 (Figure 2). Fe_2O_3 disappeared more rapidly when Cu was present; Fe_3O_4 and FeC_x were detected concurrently at shorter contact times in Fe_2O_3−Cu than in Fe_2O_3. The extent of reduction and carburization increased with time. As also shown by the CH_4 evolution isothermal transients, the induction period required to form Fe_3O_4 and FeC_x was significantly shorter on the Cu-containing sample. Also, the extent of carburization was higher on Fe_2O_3−Cu samples than on Fe_2O_3 for a given time in contact with synthesis gas. A reasonable explanation for the faster and more complete carburization of Cu-containing Fe oxides is the presence of smaller crystallites, because the rate of carburization of metal oxides is typically controlled by oxygen diffusion from the oxide core to its surface.[16] The presence of Cu metal at particle surfaces cannot possibly influence rates of oxygen diffusion through an oxide core or a carbide shell. For a given crystallite size, Fe_2O_3 and Fe_2O_3−Cu should show similar rates and extents of carburization. The apparently conflicting X-ray absorption data (Figures 2 and 4), which shows higher rates and extents of carburization on Cu-containing catalyst than on unpromoted Fe_2O_3, are reconciled by this proposal, which suggests that Cu leads to more extensive nucleation of Fe_3O_4 and FeC_x structures, leading to smaller crystallites, shorter diffusion distances, greater extent of carburization, higher surface areas, and higher hydrocarbon synthesis rates.

Product Evolution during Isothermal Transients of FeC_x-Cu and Fe_3O_4-Cu in Synthesis Gas. The simultaneous formation of Fe_3O_4 and FeC_x from Fe_2O_3 or Fe_2O_3−Cu coincides with the incipient formation of gas-phase FTS products, suggesting that either Fe_3O_4 or FeC_x may provide active sites for the synthesis of hydrocarbons from H_2/CO mixtures. In an effort to elucidate the respective roles of these two structures in FTS catalysis, we examined the initial transients in Cu-containing Fe_3O_4 and FeC_x samples, synthesized before exposure to synthesis gas at 523 K, but without intervening exposure to ambient air.

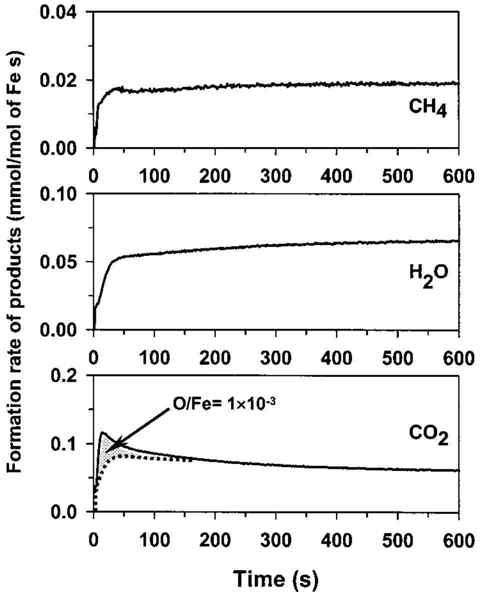

Figure 5. Rates of formation of CH_4, H_2O, and CO_2 as a function of time during contact with synthesis gas at 523 K for prereduced Fe_3O_4–Cu (0.2 g sample; Cu/Fe = 0.01; $H_2/CO = 2$, synthesis gas flow rate = 0.268 mol/h). The shaded area in the formation of CO_2 is its respective amount formed from the reduction of Fe oxides upon exposure to synthesis gas; the dashed lines is its expected values from subsequent FTS reactions.

Figure 5 shows initial rates of CH_4 formation on Fe_3O_4–Cu as a function of time in contact with synthesis gas. CH_4 formed immediately upon contact with H_2/CO, without the induction period observed on Fe_2O_3–Cu samples. The rates of CO_2 and H_2O formation were very similar to those expected from the FTS reaction itself, suggesting that Fe_3O_4–Cu became immediately active in FTS reactions upon contact with synthesis gas. CH_4 formation rates reached pseudo-steady-state values within typical turnover times (~100 s) and without significant removal of lattice oxygen. These data show that either Fe_3O_4 is the active phase during FTS reactions or that it converts, within the time required for a FTS turnover, into the required active structure, possibly surface carbide. It appears, therefore, that the assignment of activity to one of these two phases (Fe_3O_4 or a surface carbide phase derived from it) may not be provable, because their interconversion occurs in the time scale of a reaction turnover. It is inaccurate and possibly misleading to describe Fe carbides or oxides as the active phases in Fischer–Tropsch synthesis, because these two structures interconvert very rapidly in response to changes in gas phase composition. A working surface seems to be most accurately described as a dynamic phase, surrounding a thermodynamically stable oxide or carbide core, and consisting of oxygen and carbon vacancies, surface oxygen, and carbon atoms occupying lattice positions in the underlying bulk. The composition of the core appears to be irrelevant, except as an underlying matrix supporting these dynamic surface phases. The transient evolution of these surfaces in response to the relative rates of CO dissociation, carbon and oxygen removal, and hydrocarbon formation makes the relative concentrations of these species sensitively dependent on reactant composition and reaction temperature.

This somewhat disappointing but consistent picture was confirmed by measuring the evolution of products during initial contact of pre-synthesized FeC_x samples with H_2/CO reactant mixtures. If Fe_3O_4 were the exclusive active phase, initial exposure of FeC_x to synthesis gas would lead to an induction period, as the required oxygen atoms are reintroduced into the carbide structure to form Fe_3O_4, or to a much lower rate, if carbides remained as inactive or less active FeC_x species. Figure 6 shows that FeC_x samples also reached steady-state FTS rates without an induction period. Steady-state FTS rates are very similar to those obtained using Fe_3O_4–Cu and Fe_2O_3–Cu as precursors. Thus, either FeC_x surfaces provide the required FTS active sites or they convert instantaneously, within characteristic turnover times, into the required active structures. The very small amounts of oxygen ($O/Fe < 10^{-4}$) removed from Fe carbides as CO_2 during the first few seconds after exposure to synthesis gas are likely to reflect minor surface contamination of the pre-synthesized FeC_x by a trace O_2 impurity in the He carrier gas used during the time period elapsed between carbide synthesis and FTS reactions.

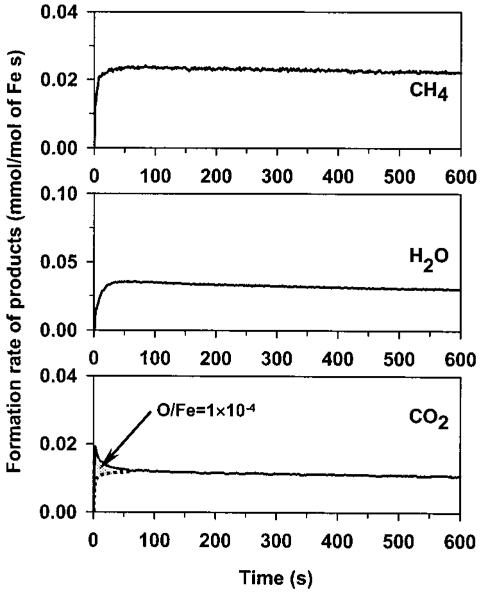

Figure 6. Rates of formation of CH_4, H_2O, and CO_2 as a function of time during contact with synthesis gas at 523 K for pre-carburized Fe_xC–Cu (0.2 g sample; Cu/Fe = 0.01; $H_2/CO = 2$, synthesis gas flow rate = 0.268 mol/h). The shaded area in the formation of CO_2 is its respective amount formed due to O_2 impurity introduced from the He carrier gas used during the time period between carbide synthesis and FTS reactions; the dashed lines is its expected values from subsequent FTS reactions.

Both Fe_3O_4 and FeC_x precursors led to the immediate attainment of similar steady-state CH_4 formation rates, without requiring any significant changes in the oxygen content of either precursor. Surface layers in either precursor reached a dynamic steady-state structure and composition upon contact with synthesis gas at 523 K. These dynamic rearrangements occur within typical turnover times; they have previously led to apparently contradictory conclusions about the active nature of Fe_3O_4 and of various Fe carbide structures in the Fischer–Tropsch synthesis. The *in situ* formation of steady-state active structures within characteristic turnover times makes definite conclusions about the active nature of various bulk species not only inaccurate, but inappropriate and potentially misleading.

These results contradict previous conclusions of Datye et al.[18,19] about the requirement for FeC_x species for FTS activity. Here, we have shown that stoichiometric Fe_2O_3, even without Cu or K and at mild FTS conditions, becomes active for FTS reactions within turnover times. The absence of hydrocarbon films around Fe_3O_4, and even the presence of spurious Fe_3O_4 crystallites, must reflect artifacts of the passivation procedures used in these *ex-situ* measurements. These passivation procedures, even when rigorously carried out, lead to local high

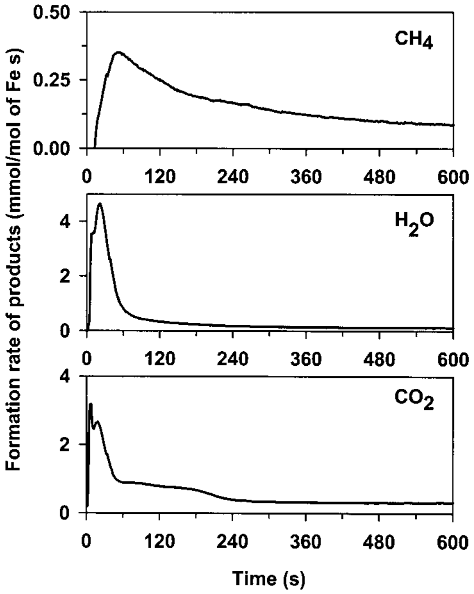

Figure 7. Rates of formation of CH_4, H_2O, and CO_2 as a function of time during contact with synthesis gas at 523 K for Fe_2O_3−K−Cu (0.2 g sample; K/Fe = 0.02, Cu/Fe = 0.01; $H_2/CO = 2$, synthesis gas flow rate = 0.268 mol/h).

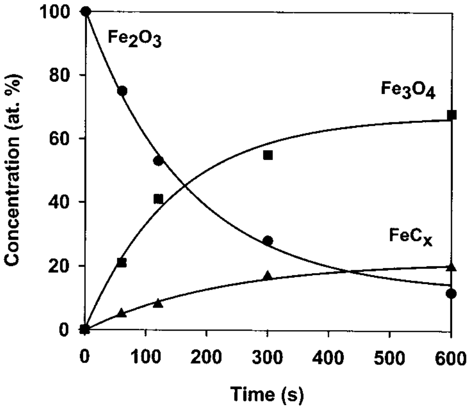

Figure 8. Structural evolution of Fe_2O_3−K−Cu with time on stream after exposure to synthesis gas at 523 K: (●) Fe_2O_3, (■) Fe_3O_4, and (▲) FeC_x (1 mg sample; K/Fe = 0.02, Cu/Fe = 0.01; $H_2/CO = 2$, synthesis gas flow rate=107 mol/mol of Fe h).

temperatures, which can combust the hydrocarbon products formed during FTS and oxidize a fraction of the FeC_x crystallites formed during FTS to Fe_3O_4.

Product Evolution and X-ray Absorption Measurements during Isothermal Transients of Fe_2O_3−Cu−K in Synthesis Gas. Figure 7 shows CH_4 evolution rates on Fe_2O_3−K−Cu (K/Fe = 0.02, Cu/Fe = 0.01) during initial contact with synthesis gas at 523 K. The rates of H_2O and CO_2 formation on Fe_2O_3−K−Cu are very similar to those measured for Fe_2O_3−Cu, except that CO becomes a more effective reductant than H_2 when K is present. The addition of K to Fe_2O_3−Cu samples led to higher rates of CH_4 formation after a short induction period, but these rates then decreased with time and reached steady-state values after ~600 s; these steady-state rates are about four times higher than on Fe_2O_3−Cu.

Near-edge Fe X-ray absorption spectra showed that the rate and the extent of carburization in Fe_2O_3−K−Cu (Figure 8) are even higher than on Fe_2O_3−Cu (Figure 4). The promotional effects of K on the rate and extent of carburization are similar to those observed when Cu was added to Fe_2O_3 precursors. Apparently K, as carbonates,[17] also provides activation sites for the synthesis gas reductant and the nucleation sites required for the formation of a larger number of smaller crystallites than in the absence of K or Cu promoters. The conclusions reached from these measurements on Fe_2O_3−K−Cu are identical to those reached from similar experiments on Fe_2O_3−Cu precursors.

TABLE 1: Surface Area and CO Chemisorption Results after 1 h FTS Reactions; Fe Carbide Concentrations Obtained from *in Situ* XAS, and CH_4 Formation Rates from Transient Experiments, on Unpromoted and Promoted Fe_2O_3 (K/Fe = 0.02, Cu/Fe = 0.01) after 5 h FTS Reactions

oxide precursor	Fe_2O_3	Fe_2O_3−Cu	Fe_2O_3−K−Cu
surface area after reaction (m^2/g)	13	17	23
amount of CO chemisorbed after reaction (mmol/mol of Fe)	8.1	14	39
steady-state FeC_x concentration[a] (at. %)	29	34	88
steady-state CH_4 formation rate[b] (mmol/g-atom Fe s)	0.061	0.070	0.19

[a] FeC_x concentration measured after exposure to synthesis gas at 523 K for 5 h (1 mg sample; $H_2/CO=2$, synthesis gas flow rate=107 mol/mol of Fe h). [b] CH_4 formation rates measured after exposure to synthesis gas at 523 K for 5 h (0.2 g sample; $H_2/CO=2$, synthesis gas flow rate=0.268 mol/h).

Promotional Effects of K and Cu on Fischer−Tropsch Synthesis Rates. BET surface areas and CO chemisorption uptakes were measured after FTS reactions for 1 h in order to confirm that K and Cu promoters led to the formation of smaller Fe carbide crystallites ($H_2/CO = 2$, 523 K; Table 1). BET surface areas were higher on samples containing K and Cu, clearly indicating the formation of smaller crystallites in activated samples. CO chemisorption uptakes were also higher on Fe_2O_3−Cu and on Fe_2O_3−K−Cu than on unpromoted Fe_2O_3. The density of binding sites available for CO chemisorption was higher on Cu-containing samples and reached the highest value when both K and Cu were present. This is consistent with the proposal that K and Cu promoters lead to the nucleation of a larger number of smaller crystallites with higher surface areas during the conversion of Fe_2O_3 precursors to Fe_3O_4 and FeC_x. FTS rates increased proportionally with the observed increase in the FeC_x content of steady-state catalysts and with the measured increase in CO chemisorption uptakes after reaction. These consistent trends among the surface area, the CO chemisorption site density, the extent of carburization, and the hydrocarbon synthesis rates indicate that the effect of K and Cu is indeed to promote the formation of smaller Fe carbide crystallites. These smaller crystallites in turn lead to a larger number of active sites for CO chemisorption, for the activation of synthesis gas during the initial structural changes of the Fe_2O_3 precursors, and thus for FTS reactions. The resulting shorter distances for oxygen transport through solid particles also lead to the more extensive carburization of Fe_2O_3 crystallites containing Cu and/or K.

These results have led to a consistent picture of the structural evolution of these materials and of its catalytic implications (Figure 9). This picture may lack some of the detailed morphological features, but it is consistent with the findings described above and with the known chemistry of oxide-carbide transformations. The shell-core structure shown schematically in Figure 9a is used to describe the reduction and carburization of Fe_2O_3 precursor crystallites in synthesis gas. Upon contact with H_2/CO at sufficiently high temperatures, lattice oxygen atoms near Fe_2O_3 surfaces are removed by reaction with H_2 or CO, to form oxygen-deficient Fe_2O_3. As the concentration of oxygen vacancies in Fe_2O_3 reaches a critical value, a new Fe_3O_4

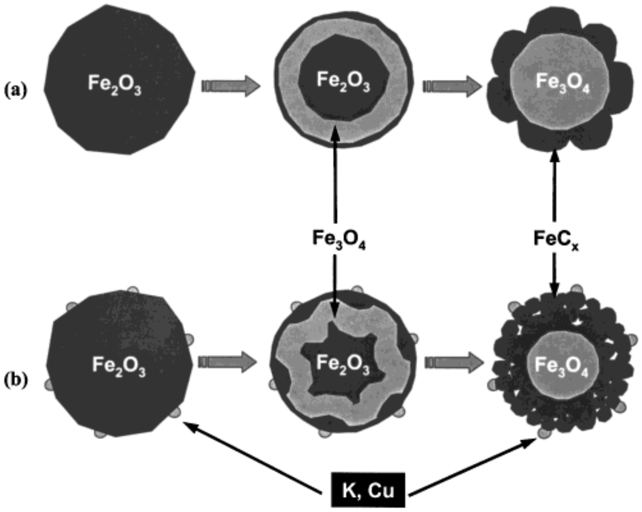

Figure 9. Shell-core model describing the structural evolution of the particles of (a) Fe_2O_3 and (b) K- or Cu-containing Fe_2O_3 after exposure to synthesis gas.

structure nucleates at the most oxygen-deficient regions, which tend to reside near Fe_2O_3 surfaces. The skeletal density of Fe_3O_4 differs only slightly from that of Fe_2O_3, but an incipient lattice mismatch can lead to the nucleation of Fe_3O_4 grains at Fe_2O_3 surfaces. This will likely occur uniformly and as a contiguous phase in unpromoted Fe_2O_3, which lack specific locations with higher oxygen deficiency. In contrast, the presence of Cu or K species at specific locations on Fe_2O_3 surfaces (Figure 9b), and their role in the activation of the H_2 and CO reactants, can lead to selected regions with higher oxygen deficiency and to the preferential nucleation of a new phase at multiple locations on the surface of an Fe_2O_3 crystallite. The nucleation of Fe_3O_4 is immediately followed by its carburization, which is likely to involve the continuing removal of lattice oxygen and the formation of oxygen vacancies leading to dissociation of CO and to the formation of carbon and oxygen species, which eventually react to form hydrocarbons and H_2O and CO_2, respectively, in the Fischer–Tropsch synthesis. This CO dissociation step leads both to progressive carburization and to FTS turnovers, thus explaining the coincident evolution of an increasingly carbided sample and of FTS catalytic activity, without implying a causal relationship between the two. As the thermodynamically favored conversion of Fe_3O_4 to FeC_x continues, a nearly uniform FeC_x shell on pure Fe_2O_3, or a patchy carbide phase on promoted Fe_2O_3, will separate from the unconverted bulk, because of significant differences in the skeletal densities of carbide and oxide structures (7.7 g/cm^3 for Fe_3C; 5.2 g/cm^3 for Fe_3O_4), and lead to the formation of Fe carbide "islands" scattered on the surface of the residual Fe_3O_4 core (Figure 9a). On K– or Cu-containing Fe_2O_3 (Figure 9b), the higher reduction and carburization rates in Fe_2O_3 regions near these promoters[2] leads to local high densities of oxygen vacancies, of Fe_3O_4 nuclei, and of carbide patches in such regions. These rapid multiple nucleation processes lead to more fractured and accessible structures, with a higher surface area, and a shorter diffusion distance for the gradual removal of the oxygen atoms retained within the remaining oxide cores. The resulting higher surface areas provide a larger number of sites for CO chemisorption and for FTS turnovers, as found in this study.

Conclusions

The removal of a small fraction of the lattice oxygen atoms in Fe_2O_3, corresponding to ~1 equivalent monolayer, is required for the formation of active sites for the Fischer–Tropsch synthesis. After these initial reduction processes, the formation of additional amounts of Fe_3O_4 and its rapid conversion to FeC_x occur without significant changes in FTS rate or selectivity. Steady-state FTS reaction rates require only the incipient conversion of the surface layers of Fe oxides to a dynamic active structure, which consists of FeC_x layers, with a catalytically irrelevant Fe oxide core, and containing a steady-state surface coverage of carbon or oxygen vacancies. Active structures form from Fe oxide precursors within characteristic turnover tines and without detectable changes in oxygen content of presynthesized Cu-containing Fe_3O_4 or FeC_x upon exposure to synthesis gas at 523 K. The facile interconversion of Fe_3O_4 and FeC_x during FTS occurs as the result of elementary steps involved in FTS and makes the assignment of catalytic activity to either of these two phases neither appropriate nor kinetically relevant. The presence of K and Cu in Fe_2O_3 precursors leads to the formation of a larger number of nucleation sites for Fe_3O_4 and FeC_x structures and to the ultimate formation of smaller crystallites. These smaller crystallites lead, in turn, to shorter diffusion paths for the conversion of the Fe_3O_4 core to FeC_x, and to a larger number of sites for CO chemisorption and for the Fischer–Tropsch synthesis reactions.

Acknowledgment. This work was supported by the U. S. Department of Energy (DOE) under Contract No. DE-FC26-98FT40308. The X-ray absorption data were collected at the Stanford Synchrotron Radiation Laboratory (SSRL), which is operated by the Department of Energy (DOE), Office of Basic Energy Sciences under contract DE-ACO3-76SF00515.

References and Notes

(1) Soled, S. L.; Iglesia, E.; Miseo, S.; DeRites, B. A.; Fiato, R. A. *Top. Catal.* **1995**, *2*, 193.

(2) Li, S.; Li, A.; Krishnamoorthy, S.; Iglesia, E. *Catal. Lett.*, in press.

(3) Li, S.; Meitzner, G. D.; Iglesia, E. *J. Phys. Chem. B* **2001**, *105*, 5743.

(4) Biloen, P.; Helle, J. N.; Sachtler, W. *J. Catal.* **1979**, *58*, 95.

(5) O'Brien, R. J.; Xu, L.; Spicer, R. L.; Bao, S.; Milburn, D. R.; Davis, B. H. *Catal. Today* **1997**, *36*, 325.

(6) Rankin, J. L.; Bartholomew, C. H. *J. Catal.* **1998**, *100*, 526.

(7) Rankin, J. L.; Bartholomew, C. H. *J. Catal.* **1998**, *100*, 533.

(8) Li, S.; Meitzner, G. D.; Iglesia, E., unpublished results.

(9) Li, S.; Krishnamoorthy, S.; Li, A.; Meitzner, G. D.; Iglesia, E., submitted to *J. Catal.*

(10) *Handbook of Chemistry and Physics*, 75th ed.; Lide, D. R., Frederikse, H. P. R., Ed.; The Chemical Rubber Company Press: Boca Raton, 1994.

(11) Bearden, A.; Burr, A. F. *Rev. Mod. Phys.* **1967**, *39*, 125.

(12) Ressler, T. J. *Synchrotron Rad.* **1998**, *5*, 118.

(13) WinXAS97 is an XAS data analysis program for PCs running MS–Windows by Thorsten Ressler (http://ourworld.compuserve.com/homepages/t_ressler).

(14) Malinowski, E. R.; Howery, D. G. In *Factor Analysis in Chemistry*; John Wiley & Sons: New York, 1981.

(15) Meitzner, G. D.; Huang, E. S. *Fresenius J. Anal. Chem.* **1992**, *342*, 61.

(16) Oyama, S. T.; Schlatter, J. C.; Metcalfe, J. E., III; Lambert, J. M., Jr. *Ind. Eng. Chem. Res.* **1988**, *27*, 1639.

(17) Li, S.; Meitzner, G. D.; Iglesia, E., unpublished results.

(18) Mansker, L. D.; Jin, Y.; Burker, D. B.; Datye, A. K. *Appl. Catal. A: General* **1999**, *186*, 277.

(19) Shroff, M. D.; Kalakkad, D. S.; Coulter, K. E.; Kohler, S. D.; Harrington, M. S.; Jackson, N. B.; Sault, A. G.; Datye, A. K. *J. Catal.* **1995**, *156*, 185.